New Ridge Flux Analysis for Fingerprint Minutiae Detection

Tomohiko Ohtsuka[1]
[1] Department of Electronics Engineering, Tokyo National College of Technology, Tokyo, 193-0997, Japan

Abstract

This paper presents a new fingerprint minutiae extraction approach that is based on the analysis of the ridge flux distribution. The considerable processing time taken by the conventional approaches, most of which use the ridge thinning process with a rather large calculation time, is a problem that has recently attracted increased attention. We observe that the features of a ridge curve are very similar to those of a vector flux such as a line of electric force or a line of magnetic force. In the proposed approach, vector flux analysis is applied to detect minutiae without using the ridge thinning process in order to reduce the computation time. The experimental results show that the proposed approach can achieve a reduction in calculation time, while achieving the same success detection rate as that of the conventional approaches.

1. Introduction

For many years, fingerprint identification has been a well known and attractive identification method. Because of the progress in the field of computers and embedded processors, fingerprint identification can now be automatically accomplished by using a stand-alone system. Fingerprint identification technology is widely used in personal recognition systems, for example, door-lock control systems and PC user management systems [1, 2].

Fingerprint representations can be broadly categorized into two types: global and local [3]. Global representation is an overall attribute of a finger; a single representation is valid for the entire fingerprint and is typically determined by an examination of the entire finger. In contrast, a local representation consists of several components, each of which is typically derived from a spatially restricted region of the fingerprint.

The most widely used local features are based on minute details called the minutiae of ridges. Localization of the minutiae in a fingerprint forms a valid and compact representation of the fingerprint. Very often in automatic fingerprint matching, only two most relevant types of minutiae are used for identification. Several approaches to local automatic minutiae extraction have already been proposed. Although rather different from one another, most of these methods transform fingerprint images into binary images through an ad hoc filtering algorithm. A thinning process is then carried out on these binary images. This process reduces the thickness of the ridge line to the width of a single pixel. Finally, a simple image scan is carried out in order to locate the pixels that correspond to the minutiae, i.e., terminations and bifurcations [3, 4, 6].

In this paper, a new minutia extraction method is proposed. This method does not contain the ridge thinning process; this elimination of the thinning process leads to a faster minutiae extraction. Since it is well known that the features of ridge curves are very similar to those of fluxes such as lines of electric force, or lines of magnetic force, it is possible to detect minutiae by using the vector analysis approach for ridge curves. In this approach, minutiae are extracted on the basis of the assumption that ridge curves have the same features as those of vector fluxes. The proposed method has low computational complexity as compared to the conventional method [3, 4] and is suitable for parallel implementation. Nowadays, as most researchers are aiming to host biometric systems onto cheap, small, portable, and low-power hardware architectures, issues related to the reduction in the computational complexity are attracting increased attention. Moreover, such architectures are characterized by low computing capabilities, limited memory, and a small biometric template size [5].

2. Overview ridge flux analysis method

2.1. Overview of conventional method

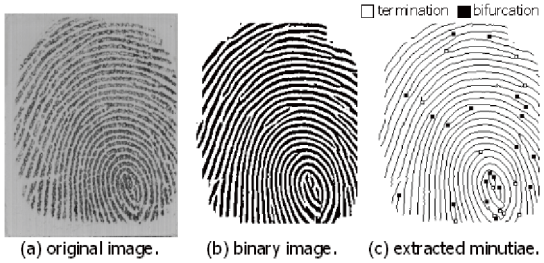

Figure 1. Overview of conventional approach.

Most automatic systems for fingerprint comparison are based on minutiae matching; hence, fast and reliable minutiae extraction is an extremely important task, and considerable research has been devoted to this topic. Although rather different from one another, most conventional methods require the conversion of a grayscale image of a fingerprint into a binary image. Some binarization processes greatly benefit from a priori enhancement. In contrast, some enhanced algorithms directly produce a binary output, and therefore, the distinction between enhancement and binarization is sometimes faded. The binary images obtained by the binarization process are usually submitted to a thinning stage, which allows the thickness of the ridge line to be reduced to one pixel. Finally, a simple image scan allows the selection of pixels that correspond to the minutiae. An overview of the conventional approach [3, 4] is shown in Fig. 1.

2.2. Basic concept of ridge flux analysis method

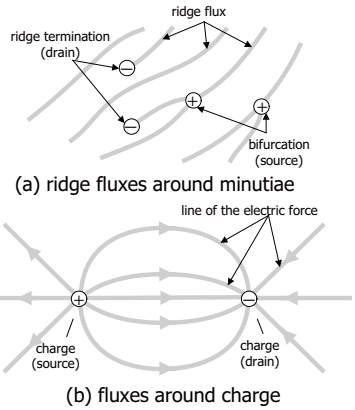

Figure 2. Similarity between ridge fluxes and lines of electric force.

The pattern of a ridge curve is very similar to that of a vector flux. Fig. 2 shows a comparison between the pattern of a ridge flux and the pattern of a line of electric force. It can be regarded that the ridge curve is generated from the bifurcation (the flux source) and is terminated at the terminal (the flux drain), as shown in Fig. 2 (a). Similarly, the line of electric force is generated from the plus charge (the line source of electric force) and is terminated at the minus charge (the line drain of electric force). In our investigations [7, 8, 9, 10], we have found that there are similar features between a ridge curve and a vector flux. In this paper, we have assumed that minutiae can be precisely detected by using a vector analysis approach called the ridge flux analysis.

2.3. Outline of ridge flux analysis method

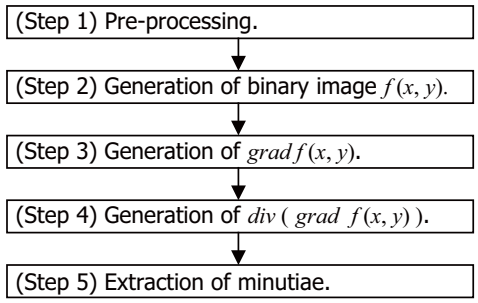

Figure 3. Outline of ridge flux analysis method.

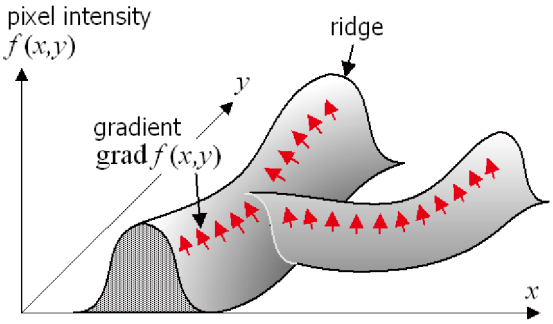

Figure 4. Ridge and its gradient.

An outline of the ridge flux analysis is shown in Fig. 3. There are five steps, i.e., pre-processing, binarization, generation of the gradient vector grad $f(x, y)$, generation of the divergence image div (grad $f(x, y)$), and minutiae extraction.

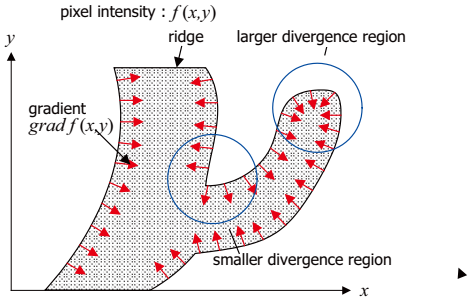

Figure 5. Projection of grad $f(x, y)$ around a terminal and a bifurcation.

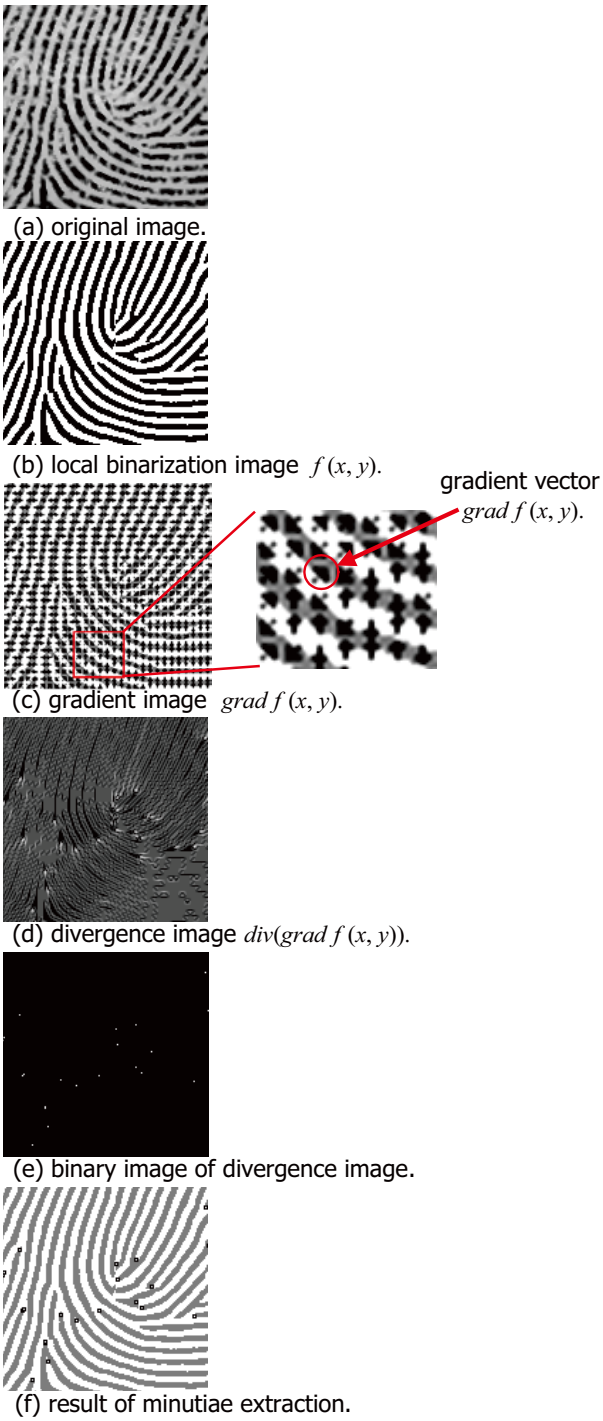

Figure 6. An example of the result image at each step in Figure 4.

In Step 1, the average filtering, the detection of the ridge direction, and the directional filtering along the

ridge direction are carried out in order to enhance the image quality [1, 2, 3].

In Step 2, the pre-processed grayscale image is separated into several small rectangle blocks, and the binary image $f(x, y)$ from the pre-processed grayscale image is generated by the local binarization for each block; this binarization is based on the assumption that the average of the pixel value can be considered to be the threshold for each block.

In Step 3, the gradient image (vector) grad $f(x, y)$ is generated from the binary image $f(x, y)$. The relation between grad $f(x, y)$ and $f(x, y)$ is shown in Fig. 4. Mathematical expression of grad $f(x, y)$ can be represented as

$$\text{grad } f(x,y) = \left(\frac{\partial f(x,y)}{\partial x}, \quad \frac{\partial f(x,y)}{\partial y} \right)^t$$

Since the derivative can be approximately represented by a linear approximation, the differential value along the x axis can be represented using $\Delta_x(x, y)$ as

$$\begin{aligned} \frac{\partial f(x,y)}{\partial x} &\approx \quad \Delta_x(x,y) \\ &= \quad k_x\left[\{f(x+1,y-1)-f(x-1,y-1)\}\right. \\ &\quad +2\{f(x+1,y)-f(x-1,y)\} \\ &\quad \left.+\{f(x+1,y+1)-f(x-1,y+1)\}\right] \end{aligned}$$

where k_x is the specified constant value. Similarly, the differential value along the y axis can be represented using $\Delta_y(x, y)$ as

$$\begin{aligned} \frac{\partial f(x,y)}{\partial y} &\approx \quad \Delta_y(x,y) \\ &= \quad k_y\left[\{f(x-1,y+1)-f(x-1,y-1)\}\right. \\ &\quad +2\{f(x,y+1)-f(x,y-1)\} \\ &\quad \left.+\{f(x+1,y+1)-f(x+1,y-1)\}\right] \end{aligned}$$

where k_y is the specified constant value. This means that a *Sobel* filter can acquire the average of each differential value along both the x direction and the y direction. These *Sobel* filters can output elements in both x and y directions of the gradient image grad $f(x, y)$.

In Step 4, the divergence image div (grad $f(x, y)$) of the gradient image vector grad $f(x, y)$ is generated in order to find locations that have a high probability of the existence of minutiae. On the basis of this investigation, we have concluded that the divergent image div (grad $f(x, y)$) has a relatively high value around the location where a termination point of ridges is relatively closer. Further, it tends to have a relatively small value when a bifurcation is close. The relationship between the gradient image grad $f(x, y)$ and the divergence image div (grad $f(x, y)$) is shown in Fig. 5. The value of div (grad $f(x, y)$) can be represented as

$$\text{div}\left(\text{grad } f(x,y)\right) = \frac{\partial^2 f(x,y)}{\partial x^2} + \frac{\partial^2 f(x,y)}{\partial y^2}$$

Using the linear approximation, we can represent $\Pi(x, y)$,

$$\begin{aligned} \text{div}\left(\text{grad } f(x,y)\right) &\approx \quad \Pi(x,y) \\ &= \quad k_x\left[\{\Delta_x(x+1,y-1)-\Delta_x(x-1,y-1)\}\right. \\ &\quad +2\{\Delta_x(x+1,y)-\Delta_x(x-1,y)\} \\ &\quad \left.+\{\Delta_x(x+1,y+1)-\Delta_x(x-1,y+1)\}\right] \\ &\quad +k_y\left[\{\Delta_y(x-1,y+1)-\Delta_y(x-1,y-1)\}\right. \\ &\quad +2\{\Delta_y(x,y+1)-\Delta_y(x,y-1)\} \\ &\quad \left.+\{\Delta_y(x+1,y+1)-\Delta_y(x+1,y-1)\}\right] \end{aligned}$$

where k_x, k_y is the specified constant value.

In Step 5, the minutiae location is extracted by using the binarization of divergence image div (grad f (x, y)); this binarization is based on the given threshold value.

An example of each output from every step is shown in Fig. 6. Fig. 6 (a) is an original fingerprint image, and Fig. 6 (b) is the binary image f (x, y) generated from the image shown in Fig. 6 (a) by applying an ad hoc filter in order to improve the image quality. Fig. 6 (c) shows the projection to the x-y plane of the gradient image grad $f(x, y)$. Both the x coordinate and the y coordinate are calculated using the *Sobel* filter. Fig. 6 (d) shows the divergence image div (grad $f(x, y)$) generated from Fig. 6 (c). Fig. 6 (d) is the binary image of div (grad $f(x, y)$), which is generated by the binarization based on the given threshold T_h by the trial-and-error approach. White dots indicate the minutiae point, where the absolute value of div (grad $f(x, y)$) becomes relatively high. In the next section, the effect of the amplitude of T_h is discussed. The final result of the minutiae extraction is shown in Fig. 6 (f).

3. Experimental results

3.1. Optimization of the threshold value of minutiae detection

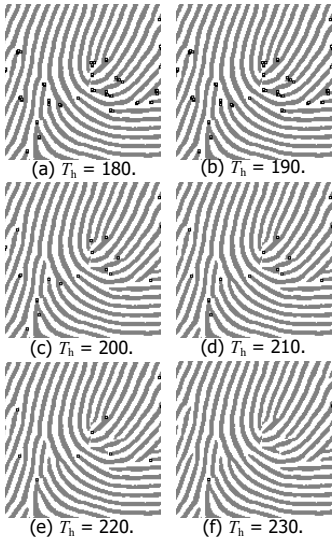

Figure 7. Minutiae detection results on threshold T_h.

It is very important to optimize the value of the threshold T_h for the binarization of the divergence image. In order to find the optimal value of the threshold T_h, we

varied its value from 180 to 230 in steps of 10 and investigated the binary image of each divergence image. Fig. 7 shows the results of the binarization based on the threshold T_h. When T_h is small, there are several white dots around the minutiae, as shown in Fig. 7 (a) and Fig. 7 (b). In contrast, several minutiae cannot be extracted when T_h is large. This means that there exists an optimal value of T_h for the minutiae extraction. On the basis of our investigation, we calculated the optimal value of T_h to be 200 for this example.

3.2. Example result of minutiae detection

Figure 8. example results of minutiae extraction using FVC2000 DB2a.

Table 1 summary of comparision of R_{detect}, R_{false} and R_{missed} for 10 fingerprints in FVC2000 DB2a.

approach	R_{detect} [%]	R_{false} [%]	R_{missed} [%]	T_{proc} [ms]
conventional	65	21	35	260
proposed	62	23	38	56

Example results are shown in Fig. 8. In order to compare our approach with the conventional approach [3, 4], we have shown the original image and the result by the conventional approach in Fig. 8 (a) and Fig. 8 (b), respectively. If there are several minutiae which are placed adjacently, the center location of adjacent minutiae is determined as the truth location of the correct minutiae location. All minutiae are extracted correctly in the results by both the conventional approach and the proposed approach. The average of R_{detect}, R_{false} and R_{missed} for 10 fingerprints in FVC2000 DB2a are summarized in Table 1. This indicates that the success detection rate of truth minutiae (R_{detect}) by proposed approach is a little lower than that of conventional approach. Both of the false detection rate of minutiae (R_{false}) and the missed detection rate of minutiae (R_{missed}) are a little higher than that of conventional approach. However the average of processing time (T_{proc}) taken to extract minutiae by the conventional approach [3, 4] using Pentium Dual Core 3.2 [GHz] Windows XP PC with 1 [GB] DRAM is 260 [ms], while the processing time in the case of the ridge flux analysis is 56 [ms]. This shows that the proposed approach is faster than the conventional approach and that it achieves almost same success detection rate of minutiae as that of the conventional approach, without carrying out the thinning process.

4. Conclusion

This paper presents a new fingerprint minutiae extraction approach that uses a ridge flux analysis. During our investigations, we observed that the features of the ridge curve were very similar to those of a vector flux such as a line of electric force or a line of magnetic force. In this approach, vector flux analysis is applied to detect minutiae without using the ridge thinning process in order to reduce the computation time. The experimental results show that the proposed approach can achieve a reduction in the calculation time, while achieving a success detection rate that is the same as that obtained by using the conventional approaches.

References

[1] S. Ozaki, T. Matsumoto, H. Imai, “Personal Verification Method Using Small Pieces of Fingerprint,” IEICE Trans. D-II, Vol. J78-D-II, no. 9, pp. 1325–1333, 1995.

[2] Y. Seto, M. Mimura, “Standardization of Accuracy Evaluation for Biometric Authentication in Japan,” IEICE Trans. ED, Vol. E84-D, no. 7, pp. 800–805, 2001.

[3] D. Simon-Zorita, J. Ortrga-Garcia, S. Cruz-Lianas, J Gonzalez-Rodriguez, “Minutiae Extraction Scheme for Fingerprint Recognition Systems,” Proc. of ICIP 2001, Vol. 3, pp.254–257, 7–10, Oct. 2001.

[4] L. Hong, Y. Wan, A. Jain, “Fingerprint Image Enhancement: Algorithm and Performance Evaluation,” IEEE Trans. Pattern Anal. Machine Intell., Vol. 20, No. 8, pp.777–789,1998.

[5] D. Maio, D. Maltone, R. Cappelli, J. L. Wayman, A. K. Jain, “FVC2004: Third Fingerprint Verification Competition,” LNCS, Springer-Verlag, 2004.

[6] D. Maltoni, D. Maio, A. K. Jain, S. Prabhakar, “Handbook of Fingerprint Recognition,” Springer, NY, 2003.

[7] T. Ohtsuka, T. Takahashi, “A New Detection Approach for Fingerprint Core Location Using Extended Relational Graph,” IEICE Trans. ED, Vol. E88D, no. 10, pp. 2308–2312, 2005.

[8] T. Ohtsuka, A. Kondo, “A New Approach to Detect Core and Delta of the Fingerprint Using Extended Relational Graph,” IEEE Proc. of 2005 ICIP, Vol. 3, pp. 249–252, 2005.

[9] T. Ohtsuka, A. Kondo, “A New Core and Delta Detection for Fingerprints Using the Extended Relation Graph,” IEICE Tran. EA, Vol. E88-A, no. 10, pp. 2587–2592, 2005.

[10] T. Ohtsuka, D. Watanabe, D. Tomizawa, Y. Hasegawa, H. Aoki, “Reliable Detection of Core and Delta in Fingerprints by Using Singular Candidate Method,” Proc. of IEEE CVPR Workshop on Biometrics, pp. 1–6, June, 2008.